Available online at www.sciencedirect.com
ScienceDirect
International Journal of Thermal Sciences 46 (2007) 308–317
International Journal of Thermal Sciences
www.elsevier.com/locate/ijts

Wind tunnel simulation of exhaust recirculation in an air-cooling system at a large power plant

Zhifu Gu [a,*], Xuerei Chen [a], William Lubitz [b], Yan Li [a], Wenlin Luo [a]

[a] *State Key Laboratory of Turbulence and Complex Systems, Department of Mechanics and Aerospace Engineering, College of Engineering, Peking University, Beijing, 100871, People's Republic of China*

[b] *Department of Mechanical and Aeronautical Engineering, University of California, Davis, CA, 95616, USA*

Received 8 August 2005; received in revised form 7 April 2006; accepted 12 April 2006

Available online 5 June 2006

Abstract

The recirculation of hot exhaust air and its dependence on wind direction was investigated as a cause of reduced efficiency in an air-cooled condenser (ACC). A method of simulating exhaust air recirculation at an ACC platform using a wind tunnel is presented, and applied to a proposed ACC addition at an existing power plant. It was found that wind speed and the height of an ACC platform have a significant impact on recirculation. Wind direction was also found to be significant, due to the interference of the buildings adjacent to the ACC platform. The mechanisms that cause recirculation are presented and analyzed, and the characteristics of the recirculating flow are described. It was found that when considering additions to existing power plants, the distance of the new ACC and power plant from the original buildings and structures has only a minor effect on the recirculation of the added ACC platform. Wind tunnel simulation is recommended in the initial design stage of new or renovated power plants with ACC systems to minimize exhaust recirculation.

Keywords: Air-cooled condenser; Wind tunnel simulation; Recirculation; Power plant

1. Introduction

A lack of an assured supply of water can be an obstacle to the construction of mine-mouth power stations in many areas of the world, particularly in northern China where coal reserves are abundant. Direct Dry Cooling Systems technology is an important solution to minimize power station water consumption.

The core device in a Direct Dry Cooling system is an air-cooled condenser (ACC). The ACC uses a space-saving A-frame design installed at level of 40 to 45 m high for a typical 600 MW power plant. The condensers are constructed with rugged galvanized steel elliptical finned tubes, which transfer heat consistently and reliably. In an ACC cell, steam exhausted from the turbine flows inside the steel elliptical finned tubes, while cooling air is drawn upward across the fins by a large fan that is mounted underneath. The cooling air removes heat from the turbine exhaust steam, causing the steam to condense. Fig. 1 shows a typical ACC cell. Under ideal conditions (i.e. with no adverse wind effects) turbine backpressure control is easily maintained by varying the airflow through the condenser.

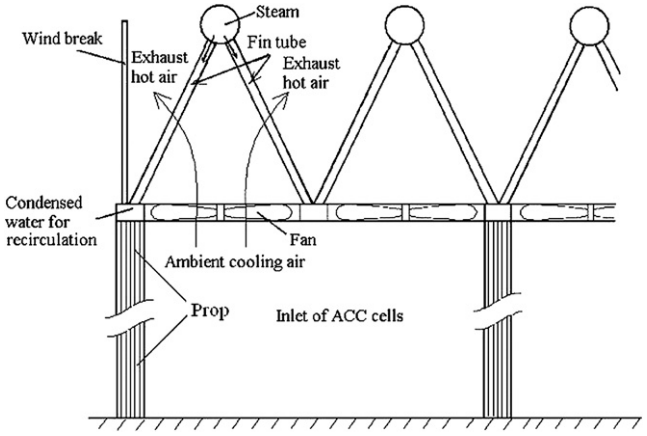

Fig. 1. Schematic drawing of an ACC cell and platform.

* Corresponding author. Tel./fax: (+86) 10 6275 6079.
E-mail address: guzf@pku.edu.cn (Z. Gu).

1290-0729/$ – see front matter
doi:10.1016/j.ijthermalsci.2006.04.007

Nomenclature

C	concentration	ppm
$\overline{C}$	averaged concentration	ppm
I	selected air inlet cell number for sampling, $= 1, 2, 3, \ldots, 64$	
L	characteristic length	m
$(F_r)_d$	densimetric Froude number, $= \frac{U}{\sqrt{gL\frac{\Delta\rho}{\rho}}}$	
g	gravitational acceleration	$\mathrm{m\,s^{-2}}$
p	pressure, $\mathrm{N\,m^{-2}}$, according to the perfect gas theorem, $= \rho RT$	
R	dimensionless recirculation	%
T	temperature	K
ΔT	temperature difference between hot exhaust air and ambient air	K
u_e	velocity of hot exhaust air from ACC	$\mathrm{m\,s^{-1}}$
U	velocity of oncoming flow	$\mathrm{m\,s^{-1}}$
z_o	surface roughness	cm

Greek letters

β	wind direction angle in degrees	°
ρ	density	$\mathrm{kg\,m^{-3}}$
$\Delta\rho$	density difference between a special gas and ambient air	$\mathrm{kg\,m^{-3}}$

Subscripts

a	ambient
c	concentration
e	hot exhaust air
m	model
p	prototype
R	recirculation
T	total

Abbreviations

ACC	Air-Cooled Condenser
ABLWT	Atmospheric Boundary Layer Wind Tunnel
ppm	Parts per million

Depending on the required capacity of the power plant, several or even hundreds of ACC cells are installed in a large rectangular platform. In small plants, the ACC platform is usually placed on top of the boiler house to avoid unfavorable wind effects. However, at larger power plants, it is impossible to place the ACC platform on the top of the buildings, due to the large size of the platform and the height of boiler houses. However, the ACC platform must be located close to the steam turbine house to maintain the efficiency of the power plant. For example, at the Matimba power plant (6 units of 665 MW each) in South Africa, the ACC platform is located just behind, and at the same height as, the steam-turbine house. This layout is typical of a large power plant using an ACC system. Problems arose at Matimba when the wind came from the direction of the buildings. Goldschagg [1] reported turbine performance at the Matimba power plant was reduced measurably during certain windy periods, and occasional turbine trips had occurred during periods of extremely gusty west winds. After extensive experimental and numerical investigations, modifications to the windbreaks and cladding were implemented. These modifications improved air flow into the air-cooled condenser during periods of westerly winds. No further trips were experienced and performance improved significantly.

Recently Kroger [2] reviewed the effect of wind on air-cooled heat exchangers and found that wind generally has a negative effect on the performance of mechanical draft heat exchangers. During windy periods, plume air recirculation tends to increase while fan performance is usually reduced. Laboratory studies and field tests have shown that the output of dry-cooled power stations may be significantly reduced by winds.

In the field of bluff body aerodynamics, when flow passes over an object on the ground, a wide region of wake flow is formed downwind. Within the wake region, part of the flow deflects downward forming a vortex that sweeps the ground in a reverse flow. When the steam turbine house and other buildings are upwind of the ACC, a large wake structure is formed in the area where the ACC is located. The result is that part of the hot exhaust air from the ACC returns to the inlet region of the condensers. If a large amount hot exhaust air recirculation takes place, a significant increase in the ACC inlet air temperature will result, greatly reducing the efficiency of the ACC.

Kroger [2] found that nearby flow interaction between an air-cooled heat exchanger and adjacent buildings or structures can significantly complicate flow patterns and reduce plant performance. For economic and safety purposes, therefore, it is very important to know the characteristics of the recirculation of an ACC system in the local wind climate early in the design of a large power plant. However, it is not always possible, especially in an extension to a power station, to always avoid unfavorable wind conditions that may cause recirculation. Thus, the question of how to minimize the unfavorable effect of wind on an ACC must be considered.

An expansion project (phase III) was planned at a power plant located in Inner Mongolia, northern China. The existing plant (phase II) used ordinary cooling towers. The expansion was planned to generate an additional 4×600 MW of electricity and to use air-cooled condensers. In this expansion, each 600 MW turbine would feed 56 ACC cells arranged in an 8×7 configuration. The ACC cells for the four turbines would be installed in a large rectangular 320 m $\times$ 70 m ACC platform, supported by 64 cylindrical concrete posts 40 or 45 m high, arranged in a 4×16 pattern. To avoid unfavorable wind effects and increase the efficiency of the condensers, 10 m high windbreaks were planned around the platform at the level of the condensers. The configuration of the project including the phase II buildings and cooling tower, together with the defini-

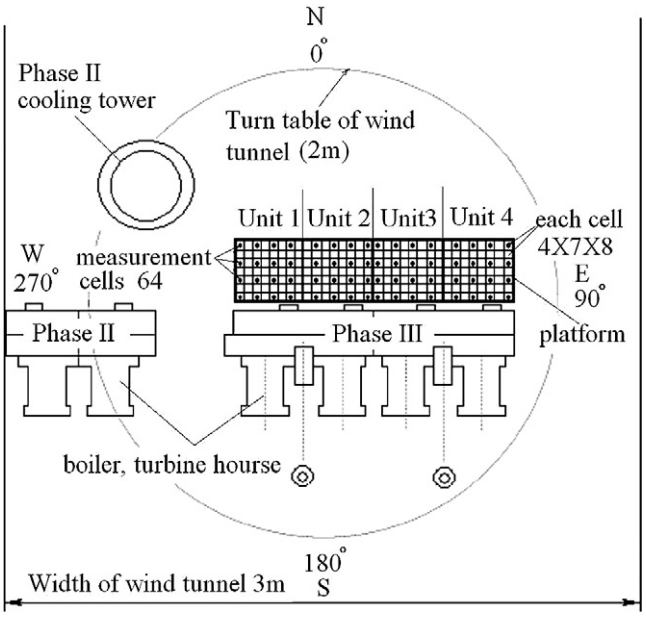

Fig. 2. Schematic showing the proposed power plant expansion (phase III) and adjacent existing plant (phase II), as well as the definition of the wind direction angle β. Black dots indicate cells where concentration measurements were recorded.

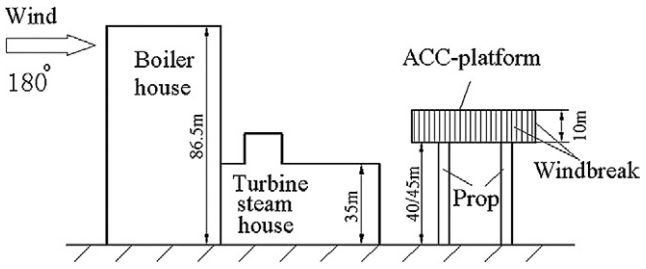

Fig. 3. Side view schematic of the boiler houses, steam-turbine house and the ACC platform.

tion of wind direction angle β is shown in Fig. 2. Fig. 3 shows a side view of the power plant including the boiler house, steam-turbine house and the ACC platform.

Since the recirculation of hot exhaust air plays a critical role in the efficiency of an ACC system, the specific properties of the recirculation flow under various conditions were investigated by means of wind tunnel simulation. This was done to better understand the characteristics, as well as the mechanisms, of wind effects on the performance of the ACC in this project. Concentration measurements of a tracer gas were taken to quantify the degree of recirculation. Flow visualizations using smoke-wire technology was also carried out to help understand the mechanisms causing occurrence of recirculation.

2. Experimental equipments, model and similarity parameters

2.1. Experimental equipments

Experiments were conducted in an atmospheric boundary layer wind tunnel (ABLWT) at Peking University, in Beijing,

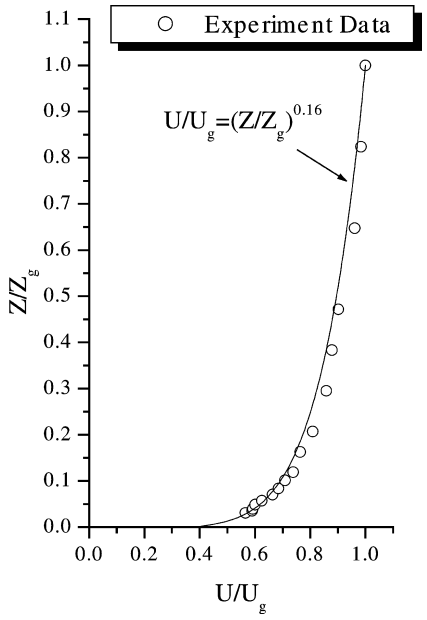

Fig. 4. Mean wind speed profile measured at the center of the turntable in the test section of the wind tunnel with no models present.

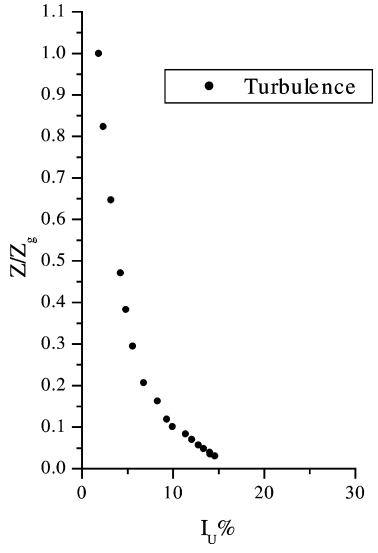

Fig. 5. Longitudinal turbulence intensity profile obtained at the center of the turntable in the test section of the wind tunnel with no models present.

China. The tunnel has a rectangular flow development section 3 m wide, 2 m high and 32 m long. A 2 m diameter turntable is located immediately downstream in the test section. The wind speed can be varied from 0.3 m s^{-1} to 10 m s^{-1}. The wind tunnel ceiling is adjustable, allowing a zero pressure gradient flow to be maintained. To simulate the atmospheric boundary layer with proper mean wind speed profiles and distributions of turbulence intensity, five spires were placed upwind, and roughness elements made from 30 mm wood cubes were arranged on the floor of the development section at 75 mm intervals. The thickness of the resulting boundary layer was about 1.5 m high. The mean wind speed and turbulence intensity profiles measured at the center of the turntable are shown in Figs. 4 and 5 respectively.

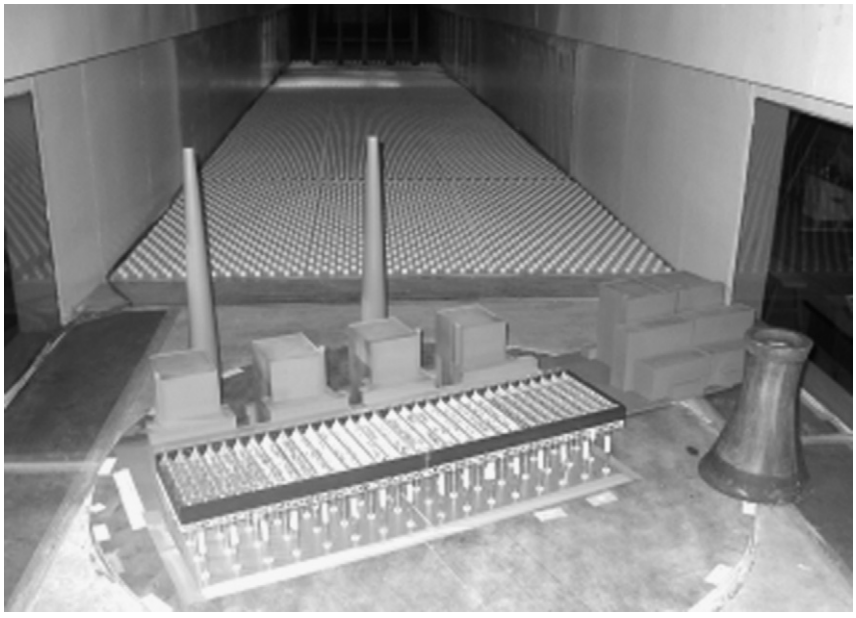

Fig. 6. Model of phase III (center) and phase 2 (right) structures in the test section of the wind tunnel. The flow development section used to generate the simulated boundary layer is also visible.

A model of the power plant, including the ACC platform, the boiler houses and the steam-turbine house, were placed on the turntable. A picture of the model installed in the wind tunnel test section is shown in Fig. 6.

The flow visualization experiments were conducted in another low speed wind tunnel at the same university. This tunnel had an open circular test section 2.25 m in diameter and 3.65 m long. The flow development section of the tunnel was modified to simulate the atmospheric boundary layer by installing a horizontal wood plate, which extends upwind through the throat of the tunnel into the upwind contraction chamber. Spires and roughness elements were placed on the plate. This configuration produced a simulated atmospheric boundary layer with a suitable depth of 1.2 m at the test section. The same models (Fig. 6) were installed in this tunnel, along with the smoke-wires for flow visualization.

2.2. The model

According to Isyumov [3], correcting for the effects of flow distortion due to tunnel blockage is difficult. However, for blockage ratios (model to wind tunnel cross-sectional area) of 5% or less, distortion effects are negligible and a correction for the speed-up of flow at the model is sufficient. A geometric model scale of 1 : 275 was selected, giving a blockage ratio of about 5.6%. To correct for speed-up of flow at the model area, the ceiling height was locally raised above the model, with gentle slopes upwind and downwind of the model. No other corrections for blockage effects were performed on the experimental data.

Models of the ACC platform were carefully constructed. To simulate the flow resistance of fin tube heat exchangers, suitable stainless steel screens were used to form the A-frame condensers. A total of 224 micro-fans, originally designed for use in notebook computers, were installed in the model to maintain the correct volume flow rate through the model condensers.

2.3. The similarity parameters

To simulate gas dispersion in a flow field in an ABLWT, several important similarity criteria must be met. It is necessary to model the characteristics of naturally occurring wind, and the dynamic and thermal properties of the exhaust plume [4]. Although this statement is for the physical modeling of stack dispersion, specifically the processes of plume rise and diffusion into the atmosphere, it is believed that the mechanisms are the same for the hot exhaust air from an ACC.

2.3.1. Jensen's criterion

Jensen's criterion must be considered [4] to properly simulate the surface boundary conditions in the wind tunnel. Essentially, the following relationship must be satisfied:

$$\frac{z_{om}}{L_m} = \frac{z_{op}}{L_p} \tag{1}$$

To obtain the proper roughness height in the wind tunnel, z_{om}, the parameters of the roughness elements, such as the element height and the spacing between elements, were carefully adjusted as described in Section 2.2, to achieve a model roughness consistent with the model scale and roughness of the prototype terrain. The power plant (prototype) is in a suburban area with $z_{op} = 20$–40 cm.

2.3.2. Densimetric Froude number

It is also necessary to model the dynamic and thermal properties of the exhaust plume. White [5] states that Froude number similarity is relatively straight-forward to achieve in a wind tunnel model; however, strict adherence to it can result in extremely low required velocities. This causes difficulties because

a critical minimum value of the Reynolds number must be maintained to ensure Reynolds-number-independent turbulent flow. Therefore, the densimetric Froude number was used,

$$(F_r)_d = \frac{U}{\sqrt{gL\frac{\Delta\rho}{\rho}}} \tag{2}$$

rather than the conventional Froude number. This can result in model wind speeds approximately 50% higher than a neutral case. This is directly related to fact that for buoyant plumes, the ratio of stack gas density to ambient air density is not unity. Although this criteria is from the physical modeling of the stack dispersion processes of plume rise and diffusion into the atmosphere, it is believed that the same mechanisms apply to the hot exhaust air from the ACC.

Applying the perfect gas theorem,

$$p = \rho RT \tag{3}$$

to Eq. (2) allows the Froude similarity relationship between the model and prototype to be written in the form,

$$\left(\frac{U}{\sqrt{gL\frac{\Delta T}{T_a}}}\right)_p = \left(\frac{U}{\sqrt{gL\frac{\Delta\rho}{\rho_e}}}\right)_m \tag{4}$$

where ΔT is the temperature difference between the exhaust hot air from ACC and ambient air, $\Delta\rho$ is the density difference between ambient air and a special gas, which will be described later, T_a is the ambient air temperature at the prototype, and ρ_e is the density of the special gas.

2.3.3. Velocity ratio between upstream wind and exhaust hot-air from ACC

To maintain a correct speed ratio of hot exhaust air velocity u_e to that of the upstream wind speed U, the following similarity must be met:

$$\left(\frac{u_e}{U}\right)_p = \left(\frac{u_e}{U}\right)_m \tag{5}$$

The exhaust hot air velocity u_e of the model was achieved by adjusting the voltage applied to the micro-fans. This was done using a precision power supply, allowing a fixed output wind speed to be produced from the fans.

Since the micro-fans were included in the ACC platform model, simulation of recirculation at the ACC during windy periods that cause inlet air flow distortions [2] could also be investigated in the experiments. Kroger [2] observed that the performance of a cooling fan can vary with ambient wind speed. Unfortunately, it was not possible to determine the impact of wind speed changes on micro-fan performance, because direct measurements of the flow velocity through the micro-fans while the wind tunnel was running were not possible. This uncertainty in the fan simulation could not be avoided. However, it is believed that since the micro-fans are in a dynamically similar environment to full scale ACC fans, performance changes due to wind effects will be similar in both the model and full scale fans. It is also expected that heat exchanger performance will be more significantly impacted by exhaust air recirculation than by variations in fan performance.

For the prototype ACC, the following thermodynamic data were assumed based on information provided by the manufacturer: volume flow rate from each of the 224 cells was 460 $m^3\,s^{-1}$, resulting in an airflow speed through the ACC cells of 2 $m\,s^{-1}$. The temperature difference between the exhaust air and the ambient air was between 30 and 33 °C.

According to Snyder [4], the concept of Reynolds number independence has been found to be extremely useful and powerful in wind tunnel simulation. Current practice indicates that sufficiently large Reynolds numbers are attainable to simulate sharp-edged geometrical structures in ordinary meteorological wind tunnels. Ricou and Spaulding [6] have shown that the entrainment rate of momentum-dominated jets in calm surroundings is essentially constant for Reynolds numbers in excess of 25 000. Only minor variations were observed between 15 000 and 25 000. Hence, if minor errors are acceptable, a critical Reynolds number of 15 000 must be maintained. Based on the characteristic length of the platform the Reynolds number for this experiment is at least 29 000, which well exceeds the critical value.

3. Measurement methods, apparatus and data reduction

To correctly simulate the dispersion of hot exhaust air from the ACC system, methane (CH_4), a special gas with a different density than air, was used to simulate the buoyancy-effect and serve as a tracer gas. The methane was released through brass tubes mounted underneath each fan. It was released at controlled flow rate, and then mixed with ambient air drawn in the model inlets by the micro-fans. The gas mixture was driven upward by the fans and passed through several layers of stainless-steel screens, which simulate the resistance of elliptical tubes. Finally the gas mixture was exhausted from the top of the condensers. This would occur at a fixed speed if there were no environmental wind effects.

Samples of the gas mixture were collected under the inlets of the ACC cells. Since it would be difficult to collect and analyze samples from all 224 cells, samples were taken from 64 selected cells that were chosen as representative of all 244 cells. The locations of the 64 cells used for concentration sampling are shown in Fig. 2. The concentration of methane in the air samples was detected and analyzed using a hydrocarbon analyzer (Backman 4000).

After measurement of the tracer gas concentration at the inlets of the ACC cells, the degree of recirculation $R_c(\beta, I)$ at a cell is calculated as

$$R_c(\beta, I) = \frac{C_R(\beta, I)}{\overline{C}_R} \quad (I = 1, 2, 3, \ldots, 64) \tag{6}$$

where $C_R(\beta, I)$ is the concentration of tracer gas sampled at inlet number I at the wind direction angle of incident flow β, and $\overline{C}_R$ is the averaged concentration of tracer gas from all condenser exhausts. To quantify the effect of the wind on the condenser recirculation at various wind directions β, the total recirculation $R_T(\beta)$ is defined as

$$R_T(\beta) = \frac{1}{64}\sum_{I=1}^{64} R_c(\beta, I) \tag{7}$$

The characteristics of recirculation may be obtained by measuring the recirculation $R_c(\beta, I)$ in the inlet of each typical cell and/or the total recirculation $R_T(\beta)$. It is understood that the quantitative relationship between the degree of recirculation and the efficiency of the ACC is a complicated question. However, it is believed that under a given set of conditions, such as for a specific wind speed, wind direction, ambient temperature and output power of the fans, the efficiency of the ACC should be inversely proportion to the recirculation. The best way to confirm this would be to perform a full-scale measurement after a power plant has been built and compare with the results of wind tunnel simulation.

4. Results and discussion

4.1. Effect of oncoming flow wind speeds and the heights of platform

It was expected that the wind speed of the oncoming flow would have a significant effect on the recirculation of exhaust air because of the change in the velocity ratio between the upstream wind and the hot exhaust air from the ACC. It was also believed that the greatest recirculation would occur when the boiler houses are directly upwind of the ACC platform ($\beta = 180°$). This was verified in later experiments on wind direction effects. Therefore the wind direction angle $\beta = 180°$ (i.e., wind comes from the south) was selected to determine the effect of wind speed on the recirculation. Wind speed measurements were available from a local weather station at a height of 10 m, and local wind climate data was available at a reference height of 10 m. Therefore, a range of wind speeds corresponding to full-scale speeds of 2.0, 4.0, 6.0, 8.0 and 10 m s^{-1} at 10 m height were used in the experiment. Since the height of the ACC platform also affects the recirculation, two different heights of the ACC platform were tested: 40 m (case 1) and 45 m (case 2). In order to examine recirculation at high wind speeds, 12 and 15 m s^{-1} winds were also tested for case 2.

The total recirculation $R_T(\beta = 180°)$ results for the two cases are shown in Fig. 7. At a wind speed of 2 m s^{-1}, the total recirculation $R_T(\beta = 180°)$ for the two cases was almost the same. As the wind speed was increased, the values of $R_T(\beta = 180°)$ increased for both cases. However, in case 1, the maximum value of $R_T(\beta = 180°) = 35.4\%$ was reached at a wind speed of 6 m s^{-1}, while in case 2, the maximum value of $R_T(\beta = 180°) = 26.8\%$ was reached at a wind speed of 8 m s^{-1}. It is clear that at wind speeds between 4 and 10 m s^{-1}, the values of $R_T(\beta = 180°)$ in case 2 are almost 30% less than the values observed in case 1. Therefore, the height of the ACC platform had a significant effect on recirculation when the wind blew from upwind of the boiler houses. As the wind speed was increased from 12 to 15 m s^{-1} in case 2, values of $R_T(\beta = 180°)$ were further reduced, but were trending to a constant non-zero value. Note that in the case of zero wind speed, Eq. (5) becomes undefined, and it is not technically possible to simulate recirculation under no wind conditions.

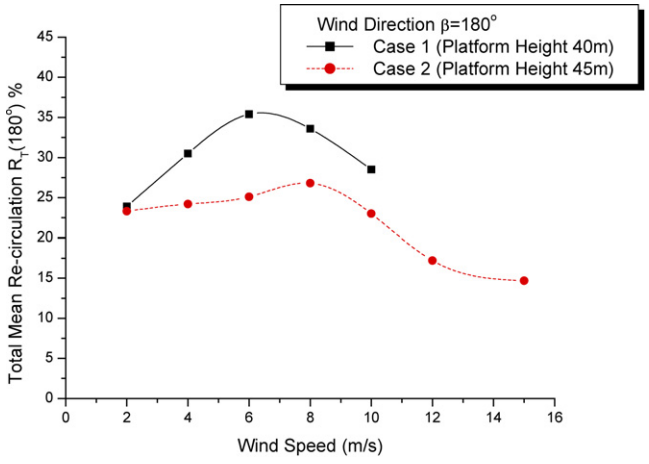

Fig. 7. Total recirculation $R_T(\beta = 180°)$ versus wind speed for two ACC platform heights.

4.2. Effect of wind directions

It is obvious that wind direction has a great effect on the recirculation due to the interference of buildings and the ACC platform. Based on the results investigating the effect of the ACC platform height, the 45 m high platform was chosen to minimize recirculation. This platform was tested for recirculation at 14 different wind directions. A wind speed of 8 m s^{-1}, corresponding to the maximum observed value of $R_T(\beta = 180°)$, was selected for the wind direction experiments. Fig. 8 shows how the total recirculation varies with the wind direction β.

A set of wind direction experiments were also carried out with no building models other than the ACC platform (i.e., phase III only) to observe the variation in recirculation with wind direction for a typical ACC power plant. It was found that when the wind blows normal to the major axis of the ACC platform (i.e. the wind comes from the side of the ACC platform) the value of $R_T(\beta)$ is quite small and the recircu-

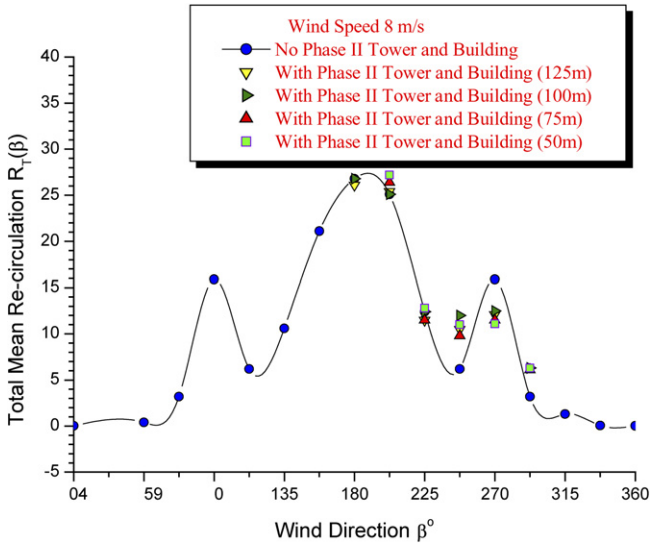

Fig. 8. Total recirculation $R_T(\beta)$ versus wind direction β for different spacing distances of the phase II and phase III structures.

lation is almost undetectable. When the power plant buildings were located downwind of the ACC platform, the interference was rather weak, and low levels of recirculation were only detected when the wind blew normal to the major axis of the ACC platform ($\beta = 0°$) or within $\pm 45°$. In these cases, the total recirculation levels were quite low, and the wind effects on the efficiency of the ACC could be ignored. However, as the wind direction became parallel to the direction of the ACC major axis (i.e., along the gap between the steam-turbine house and the ACC platform when $\beta = 90°$ or 270°) the total recirculation rose quickly, up to a peak value of $R_T(\beta) = 16\%$. Kroger [2] also found that when the wind blows in the direction of the major axis of an exchanger, recirculation of hot plume air results. The mechanism that causes this phenomenon is discussed later. As the wind angle was increased further, $R_T(\beta)$ was reduced again, reaching a value of less than 7% at $\beta = 112.5°$. As the wind angle was increased still further past 90°, the buildings gradually become located upwind of the ACC platform, and the interference again became stronger, causing the value of $R_T(\beta)$ to increase rapidly. Under these conditions, the ACC platform is partially or fully immersed in the wake region behind the turbine-steam and boiler houses. For the case with buildings upwind, it was found that the most unfavorable wind effects on the ACC occurred when the wind blew normal (i.e., $\beta = 180°$) to the boiler houses or within $\pm 22.5°$. These findings agree with laboratory studies and field tests performed by Schulenberg [7] at the Wydok power plant, where a reduction in turbine output was observed under similar wind conditions. The Wydok data showed that the output of dry-cooled power stations can be significantly reduced by winds. The greatest reduction in turbine output occurred at a relative wind direction of 180°, with two other reduction peaks of less magnitude occurring at other wind directions.

It should also be noted that in another 6×600 MW plant in China, which is similar to the Matimba 6×665 MW plant, experiments showed that the most serious recirculation occurred over the range $\beta = 180 \pm 22.5°$, rather than just when the wind blew normal to the boiler houses ($\beta = 180°$). It is clear the geometric details and arrangement of the boiler houses also play an important role in wind-induced recirculation. Since the configurations of these power plants were quite different, it is suggested that the observed impacts of wind direction on recirculation is a common phenomenon at many plants.

Detailed information about recirculation distribution across all the inlets of the ACC platform under various wind conditions were necessary to clarify the mechanisms that cause recirculation. Therefore, tests were conducted of recirculation distribution under various conditions. As an example, Fig. 9 shows a contour map of recirculation distribution across the ACC platform inlets for case 2 (45 m ACC platform) at four typical wind directions ($\beta = 0°$, 90°, 157.5° and 180°).

Generally, at $\beta = 180°$ the recirculation is high across all of the inlets of the ACC system, and is extremely high for the middle two units (unit 2 and unit 3). Additionally, the $R_T(\beta)$ peak values occur at inlets in the downwind portion of the ACC platform. This means that the amount of recirculation flow that comes from the downstream side of the ACC platform is greater than the recirculation that comes from the upwind side. This phenomenon was confirmed using flow visualization, shown in Fig. 10. This case ($\beta = 180°$) causes the highest recirculation for units 2 and 3 over all wind directions. Because air is also drawn in through the short sides of the ACC platform, the performance of the end units (unit 1 and unit 4) was better relative to the middle two units.

Flow visualizations using the smoke-wire method were also carried out for several typical cases. Fig. 10 shows a visualization of the most serious recirculation, which occurred when the boiler house was upwind ($\beta = 180°$), at a simulated full-scale wind speed of 8 $\mathrm{m\,s^{-1}}$, and a typical full-scale design exhaust air speed from the fans of 2 $\mathrm{m\,s^{-1}}$. Four wires were arranged in a line parallel to the wind and in the plane between the two boiler houses. The first wire was located in front of the boiler house. The second wire was placed at the leeward surface of the boiler house. The third and fourth wires were located just behind the steam-turbine house and leeward of the platform, respectively. The wires were coated with oil prior to each test. During the tests, electricity was passed through the wires, heating them by electrical resistance, and causing the oil to smoke.

It can be seen that as the wind blew over the boiler house, wake flow structures were formed behind the buildings. Two strong recirculation cells were generated by the fans in the platform. Some of the air exhausted from the top of the upstream portion of the platform was drawn down into the gap between the steam-turbine house and the platform, due to the strong negative pressure field generated by the wake flow and the platform fans, and passed through the gap to the inlets of the ACC. This formed the first strong recirculation cell. On the downwind side, some of the exhaust air from the downstream portion of the platform was drawn downward by the strong negative pressure field located to the lee of the platform. This caused the second strong recirculation cell. The relative contribution of the two cells to recirculation depends on the configuration parameters (such as heights, distances, etc.) of the boiler houses, the steam-turbine house and the ACC platform. In this configuration the second (downwind) cell experienced greater recirculation than the first (upwind) cell. This agrees with the measured distribution of recirculation at the inlets of ACC platform at $\beta = 180°$, as shown in Fig. 9.

When the wind blows at $\beta = 157.5°$, the wake structures generated by the boiler houses no longer significantly affect unit 4, and the recirculation at unit 4 is rather low. While the recirculation at unit 1 is increased greatly, the total recirculation over the entire platform $R_T(\beta = 157.5°)$ is decreased relative to the $\beta = 180°$ case. However, as the wind angle turns to $\beta = 90°$ (i.e., wind blows along the gap between the steam-turbine houses and the ACC platform), $R_T(\beta)$ increases again and reaches another peak value. As shown in Fig. 9, two strong recirculation regions occur located very close to the downstream edge of the ACC windbreaks. The appearance of the strong recirculation regions can be explained by wind entrainment due to the combination of the windbreak and channel effect, which causes the strong suction field in the gap. During crosswind conditions, Fahlsing [8] observed reverse rotation of out-of-service fans on the windward side of an ACC, indicating

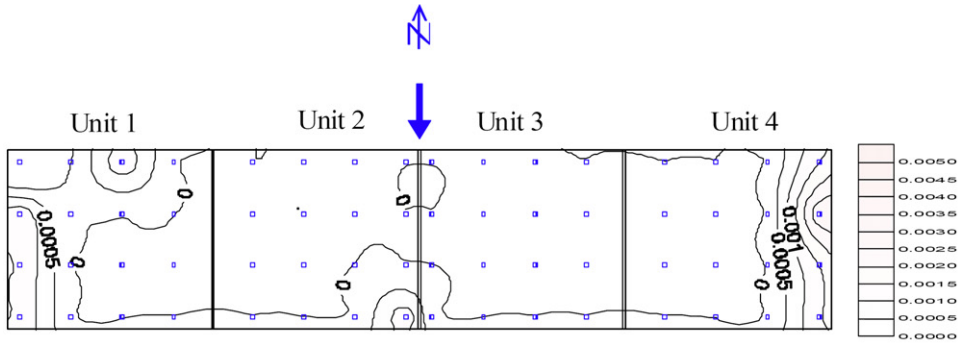

β = 0°, Average $R_T(\beta) = 0.02\%$

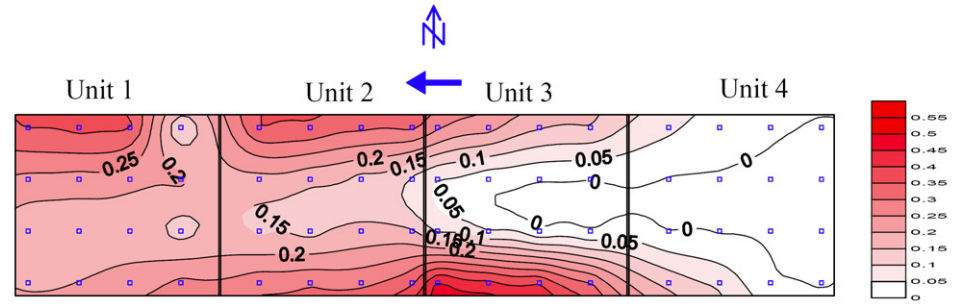

β = 90°, Average $R_T(\beta) = 15.9\%$

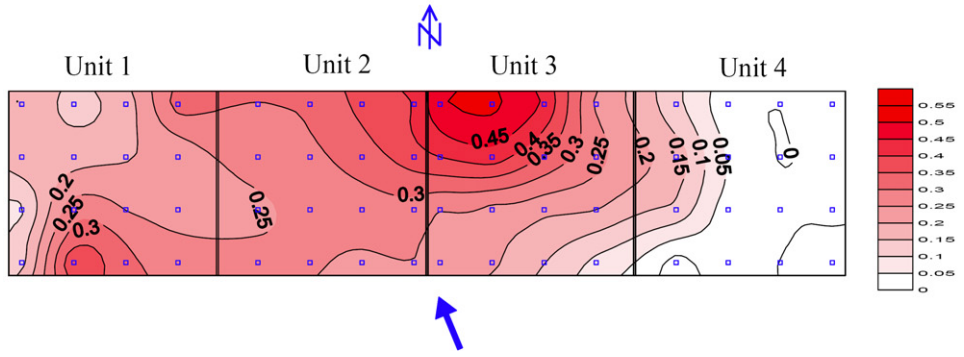

β = 157.5°, Average $R_T(\beta)$ =21.1%

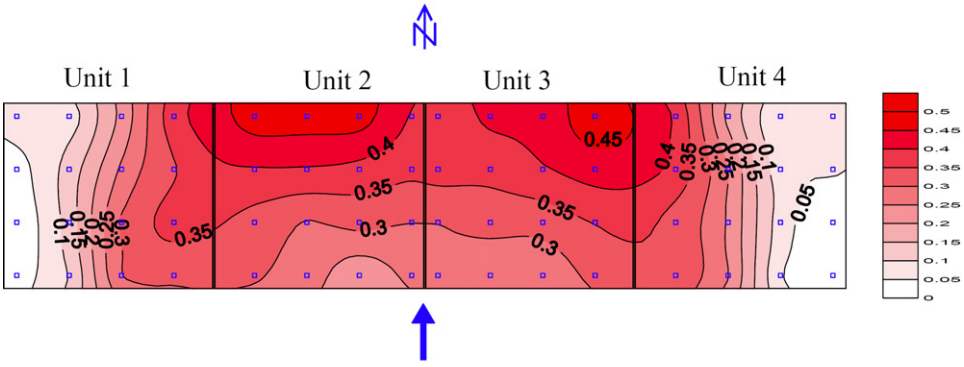

β = 180°, Average $R_T(\beta)$ =26.8%

Fig. 9. Distribution of recirculation $R_T(\beta)$ over the inlets of the ACC platform at $\beta = 0°$, 90°, 157.5° and 180°. Contour interval 0.05.

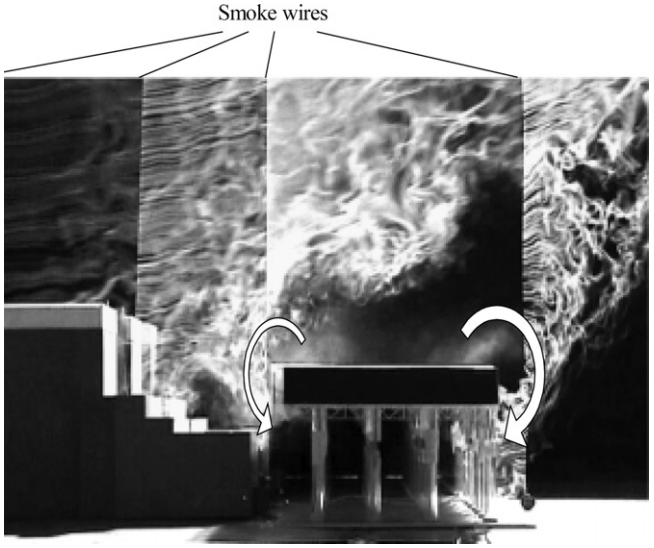

Fig. 10. Smoke wire flow visualization with the boiler houses upwind of the ACC platform ($\beta = 180°$). Wind is blowing from left to right.

reverse flow. It is believed the same phenomenon occurred in this condition. In this study, extremely high concentrations of the tracer gas were detected at several inlets located very close to the windbreak, due to reversed flow at the out-of-service fans. It should be noted that this phenomenon does not conform to the definition of recirculation, which presumes upward flow through the fans. Therefore the measurements in this special condition do not correctly represent the magnitude of the recirculation phenomenon. However, this is the most serious condition affecting the performance of local ACC cells. Finally, when the wind blows normal to the major axis of the ACC platform (i.e., wind comes from the side of the ACC platform, as shown in Fig. 9 at $\beta = 0°$), minimal recirculation can be detected.

4.3. Effect of distances between phases II and III

In order to minimize the wind effects on the planned phase III ACC platform, it was necessary to determine the recirculation impact due to the original phase II structures. One parameter to be determined was the optimal spacing between the phase II and phase III structures. Four different distances between the phase II and phase III structures were tested: 50 m, 75 m, 100 m and 125 m. It is believed that when the phase II structures are located downwind of the phase III ACC platform, there will be little recirculation. Therefore, tests were performed for five wind directions where phase II was located upwind of phase III.

Total recirculation with phase II present is plotted in Fig. 8 for each of the five tested wind directions. Even for the most impacted wind directions, the change in recirculation due to the inclusion of phase II is quite low. Changes in recirculation only occurred when the phase II structures were located upstream of the phase III ACC platform. However, the effect of the distance between phases II and III as a function of wind directions was rather complex. At some angles, $R_T(\beta)$ was even reduced relative to not including the phase II structures. At the wind angle $\beta = 247.5°$, values of $R_T(\beta)$ increased markedly, but not to a serious level. Measured values of $R_T(\beta)$ for different distances between phase II at the typical wind directions compared with that of no phase II are listed in Table 1. The results suggest that, for this project, the existence of the phase II structures will have only a minimal effect on the new ACC system.

Table 1
Values of $R_T(\beta)$ for different distances between phases II and III at several wind directions

Wind directions β		180°	202.5°	225°	247.5°	270°	292.5°
No phase II		26.1	24.1	12.5	5.4	13.9	2.7
Distance between phases II and III	125 m	26.8 ↑	25.4 ↑	11.5 ↓	10.5 ↑	12.1 ↓	6.3 ↑
	100 m		25.1 ↑	12.4 ↓	12.0 ↑	12.5 ↓	
	75 m		26.4 ↑	11.5 ↓	9.8 ↑	11.5 ↓	6.1 ↑
	50 m		27.2 ↑	12.8 ↑	11.0 ↑	11.1 ↓	6.3 ↑

$R_T(\beta)$ is also given for case without phase II structures present. Arrows indicate an increase (↑) or decrease (↓) in recirculation relative to the no phase II case (i.e., phase III only).

5. Conclusions

The recirculation parameter ($R_T(\beta)$) was introduced to investigate the effect of wind on the efficiency of ACC systems. The performance of an ACC system in a large power plant depends on many parameters, such as the local wind climate, plant configuration and the details of the ACC platform. Wind tunnel criteria for simulating exhaust air recirculation at an ACC were discussed and experimental methods were described. A proposed expansion project at a typical large power plant was studied. The characteristics of recirculation under various conditions have been presented and discussed. It was observed that recirculation caused by interference from neighboring buildings and structures can significantly reduce the efficiency of ACC as which were located in the wake of buildings and structures.

Both the wind speed and the height of the ACC platform greatly affect recirculation. When the wind blows so that the ACC is downwind of the boiler houses, the maximum recirculation reached will depend on the wind speeds and the height of the ACC platform. In this project, when the platform height was raised 5 m, the recirculation was reduced almost 30% for wind speeds between 4 and 10 m s^{-1}.

The wind direction has a significant effect on the total recirculation, as well as its distribution across the inlets of an ACC platform. Two peak values of $R_T(\beta)$ appeared, the first when the wind blew so that the boiler houses were upwind of the ACC ($\beta = 180°$), and the second when the wind direction was aligned with the gap between the steam-turbine house and the ACC platform ($\beta = 90°$ or 270°). The greatest recirculation occurred when the boiler houses were directly upwind ($\beta = 180°$) or within ±22.5°, because of the severe interference caused by the boiler house wake. On the other hand, when the wind blew in the direction of the gap between the steam-turbine house and ACC platform ($\beta = 90°$ or 270°), the serious condition of reverse flow at out-of-service fans may happen at some local ACC cells. When the ACC is upwind of the boiler houses ($\beta = 0°$), or within ±45°, only minimal recirculation could be detected. The most favorable arrangement for a power plant with an ACC

platform occurs when the prevailing local wind direction is such that the ACC is on the upwind side of the plant.

When considering additions to existing power plants, such as the case study in this investigation, the distance of the new ACC and power plant from the original buildings and structures has only a minor effect on the recirculation of the added ACC platform.

Wind tunnel simulation can be used to investigate the nature of recirculation at an ACC, and results can be used to reduce unfavorable wind effects on ACC platforms. Therefore, wind tunnel simulation could play an important role during the initial design stage of new power plants, or additions to existing plants, with ACC systems. Wind tunnel measurements, combined with information on the local wind climate, can result in more reasonable, economic and safe power plant designs.

Acknowledgements

This project was partly supported by National Natural Science Foundation of China (10172008).

References

[1] H. Goldschagg, Winds of change at Eskom's Matimba plant, Modern Power Systems, 43–45, January 1999.
[2] D. Kroger, Air-Cooled Heat Exchangers and Cooling Towers; Thermal-Flow Performance Evaluation and Design, vol. 2, PennWell Publishing Company, 2004.
[3] N. Isyumov, Wind Tunnel Studies of Buildings and Structures, ASCE Manuals and Reports on Engineering Practice, vol. 67, 1999.
[4] W.H. Snyder, Guideline for fluid modeling of atmospheric diffusion, US EPA Rpt. No. EPA-600/8-81-009, 1981.
[5] B.R. White, Physical modeling of atmospheric flow and environmental applications, in: Proceedings of the 51st Anniversary Conference of KSME 1996, Pusan National University, Pusan, Korea, April 19–20, 1996.
[6] F.P. Ricou, D.B. Spalding, Measurement of entrainment of axisymmetrical turbulent jets, J. Fluid Mech. 11 (1961) 21–32.
[7] F.J. Schulenberg, Steam condensation in the utility industry using air-cooled heat exchangers, Paper, Power Utility Industry, Hiroshima, Japan, 1976.
[8] P.M. Fahlsing, Benefits of variable speed drives applied on dry condensing at the Wyodak plant, in: Proceedings, American Society of Mechanical Engineers Joint Power Generation Conference, PWR-28:463-471, October 1995.